Dead-time correction of fluorescence lifetime measurements and fluorescence lifetime imaging

Sebastian Isbaner,[1,3] **Narain Karedla,**[1,2,3] **Daja Ruhlandt,**[1] **Simon Christoph Stein,**[1] **Anna Chizhik,**[1] **Ingo Gregor,**[1] **and Jörg Enderlein**[1,2,*]

[1]*III. Institute of Physics, Georg August University, Friedrich-Hund-Platz 1, 37077 Göttingen, Germany*
[2]*DFG Research Center "Nanoscale Microscopy and Molecular Physiology of the Brain" (CNMPB), Göttingen, Germany*
[3]*equally contributing authors*

[*]*jenderl@gwdg.de*

http://www.joerg-enderlein.de

Abstract: We present a comprehensive theory of dead-time effects on Time-Correlated Single Photon Counting (TCSPC) as used for fluorescence lifetime measurements, and develop a correction algorithm to remove these artifacts. We apply this algorithm to fluorescence lifetime measurements as well as to Fluorescence Lifetime Imaging Microscopy (FLIM), where rapid data acquisition is necessarily connected with high count rates. There, dead-time effects cannot be neglected, and lead to distortions in the observed lifetime image. The algorithm is quite general and completely independent of the particular nature of the measured signal. It can also be applied to any other single-event counting measurement with detector and/or electronics dead-time.

OCIS codes: (170.2520) Fluorescence microscopy; (170.6920) Time-resolved imaging.

References and links

1. U. Kubitscheck, *Fluorescence Microscopy: From Principles to Biological Applications* (Wiley-VCH, 2013).
2. P. P. Mondial and A. Diaspro, *Fundamentals of Fluorescence Microscopy: Exploring Life with Light* (Springer, 2014).
3. K. R. Spring and M. W. Davidson, "Introduction to Fluorescence Microscopy," http://www.microscopyu.com.
4. T. Niehörster, A. Löschberger, I. Gregor, B. Krämer, H.-J. Rahn, M. Patting, F. Koberling, J. Enderlein, and M. Sauer, "Multi-target spectrally resolved fluorescence lifetime imaging microscopy," Nature Methods **13**(3), 257–262 (2016).
5. R. M. Clegg, "Fluorescence resonance energy transfer," Curr. Opin. Biotechnol. **6**, 103–110 (1995).
6. R. M. Clegg, "Fluorescence Resonance Energy Transfer," in *Fluorescence Imaging, Spectroscopy and Microscopy*, X. F. Wang and B. Herman, eds. (John Wiley and Sons, 1996), pp. 179–252.
7. J. B. Pawley, *Handbook of Biological Confocal Microscopy* (Springer, 2006).
8. D. V. O'Connor and D. Phillips, *Time-correlated Single Photon Counting* (Academic Press, 1984).
9. M. Wahl, "Time-Correlated Single Photon Counting," http://www.picoquant.com/images/uploads/page/files/7253/technote_tcspc.pdf.
10. W. Becker, *Advanced Time-Correlated Single Photon Counting Techniques* (Springer, 2005).
11. M. Wahl, H.-J. Rahn, I. Gregor, R. Erdmann, and J. Enderlein, "Dead-time optimized time-correlated photon counting instrument with synchronized, independent timing channels," Rev. Sci. Instrum. **78**, 033106 (2007).

12. C. Holzapfel, "On Statistics of Time-to-Amplitude converter systems in photon counting devices," Rev. Sci. Instrum. **45**, 894-896 (1974).
13. C. C. Davis and T. A. King, "Photon pile-up corrections in the study of time-varying light sources," J Phys E: Sci Instrum. **5**, 1072 (1972).
14. M. Patting, M. Wahl, P. Kapusta, and R. Erdmann, "Dead-time effects in TCSPC data analysis," Proc. SPIE **6583**, 658307 (2007).
15. J. Arlt, D. Tyndall, B. R. Rae, D. D.-U. Li, J. A. Richardson, and R. K. Henderson, "A study of pile-up in integrated time-correlated single photon counting systems," Rev. Sci. Instrum. **84** 103105 (2013).
16. L. Fleury, J. Segura, G. Zumofen, B. Hecht, and U. P. Wild, "Photon statistics in single-molecule fluorescence at room temperature," Phys. Rev. Lett. **95**, 19–22 (2000).
17. A. McCarthy, R. J. Collins, N. J. Krichel, V. Fernandez, A. M. Wallace, and G. S. Buller, "Long-range time-of-flight scanning sensor based on high-speed time-correlated single-photon counting," Appl. Opt. **48**, 6241 (2009).
18. J. R. Lakowicz, *Principles of Fluorescence Spectroscopy* (Springer, 2013).

1. Introduction

Fluorescence microscopy has become an indispensable tool in modern biology and medicine [1–3]. This is due to the high sensitivity of fluorescence detection, but also to the selectivity with which structures of interest can be labeled. In particular the ability to label different targets with different fluorescent dyes of different spectral properties makes fluorescence microscopy such a powerful tool in studying the relative structural organization and dynamics of various parts and molecules of living cells. Besides using fluorescent dyes of different excitation/emission wavelengths and discriminating them by spectrally resolved fluorescence detection, a further means of disentangling different dyes in a fluorescence microscopy image is to use their fluorescence lifetime, see e.g. [4]. As with the spectral properties, which differ from dye to dye, also the fluorescence lifetime is different between different dyes. Moreover, fluorescence lifetime measurements have become increasingly popular for the quantification of Förster Resonance Energy Transfer (FRET) [5, 6] measurements in bio-imaging, because they allow for accurate FRET rate estimates which are independent of intensity measurements that can be skewed by optical absorption, cross-talk, and/or scattering.

In the present paper, we consider a FLIM system which is based on a confocal scanning microscope [7] and which uses TCSPC [8, 9] for measuring the fluorescence decay at every scan position. If a fluorescent molecule is excited from its electronic ground state into its first electronic excited state, it will remain, on average, for a certain time (on the order of nanoseconds) in this state before jumping back to its ground state while emitting a fluorescence photon (or via other, non-radiative de-excitation channels). The chance to find a molecule still in its excited state after excitation is described by the fluorescence decay curve. In TCSPC, one determines this curve by exciting molecules with a periodic train of short laser pulses, and then measuring the time delay between the recorded fluorescence photons and the exciting laser pulses. When building a histogram of these delay times, one obtains an estimate of the fluorescence decay curve, which is typically fitted with a single- or multi-exponential decay function. Modern TCSPC systems measure the arrival times of detected photons in an asynchronous way, independent of the laser pulse times, and only subsequently correlate recorded photon detection times with the times of the laser pulses. However, an important detail is that both the photon detector(s) as well as the timing electronics have dead-times: After a successful detection (detector) or timing (electronics) of a photon, both detector and electronics need to recover and to return to an active state before being able to detect/record the next photon. These recoveries typically take several tens of nanoseconds and, therefore, cannot be neglected. At high count rates where the time between photons is in the order of the some percent of these dead-times, this leads to an increasing loss of detectable photons, and worse, to a distortion of the finally measured fluorescence decay curve.

The distortion of dead-time effects are reduced at low count rates. Low count rates limit the

signal-to-noise ratio and increase the time to obtain sufficient statistics for a fluorescence decay curve, which in turn limits the image acquisition rate in scanning microscopy. In FLIM, at each scan position during the sample scan with a laser-scanning confocal microscope, one records a TCSPC curve from which not only the fluorescence intensity but also a lifetime value is extracted. For rapid FLIM image acquisition, one wants to maximize the count rate that should be limited only by photobleaching and phototoxicity, but not by potential dead-time effects in the TCSPC measurement. Thus, a TCSPC data evaluation method that faithfully reproduces the correct fluorescence decay curve even at high count rates is an important prerequisite for unbiased fast FLIM. Here, we present a data evaluation method which provides dead-time corrected fluorescence decay estimates from TCSPC measurements at high count rates, and we demonstrate our method on FLIM of fluorescently labeled cells.

Note that our work focuses on pure dead-time systems without pile-up and is in general not applicable to classical reverse start-stop TCSPC. We do not consider pile-up, which would complicate the description and is beyond the scope of the current work.

2. Fundamentals

2.1. Distortion effects in TCSPC measurements

In a TCSPC measurement, the arrival time of photons is measured with respect to an external sync source, usually provided by the pulsed excitation laser. The output pulse of the detector is electronically timed, typically by a Time-to-Digital Converter (TDC). Different TCSPC schemes exist:

1. In (forward) start-stop TCSPC, the laser sync starts the timer and a photon detection event stops the timer. After the stop, there will be a certain dead-time of the timing electronics. The first laser sync after the dead time starts the timer again. This means that only the first photon in an excitation period can be recorded, so there is a preference to detect the early photons of the decay, also referred to as "classical pile-up" [10].

2. In reverse start-stop TCSPC, a photon detection event starts the timer and the next sync pulse stops the timer. After the stop and the dead-time of the timing electronics, the next photon can start the timer anytime during the sync period. This leads to a lower detection probability in the beginning of the sync period, also referred to as "inter-pulse pile-up" [10]. An additional complication is that the TDC in these systems usually works by charging a capacitor with a constant current so that the voltage is proportional to the elapsed time. Since the read-out involves discharging the capacitor, the duration of the dead-time depends on the start pulse and thus on the photon arrival time [10].

3. A modern TCSPC system, such as described in [11], uses independent clock-based TDC timers for the sync and detector pulses. Only when a photon is timed, the start-stop time is recorded as the difference of the detector timer and the sync timer. For sync periods longer than the dead-time it is thus possible to record more than one photon during one sync period.

The first two described TCSPC systems have the limitation that they can detect only one photon per sync period (pile-up effect [10]). Especially the classical pile-up of forward start-stop TCSPC does not depend on the dead-time and has been adressed in several publications, see for example [12, 13], and references therein. Reverse start-stop measurements suffer from pile-up as well as dead-time distortions [14]. An overview on different start-stop TCSPC architectures and their pile-up behavior is given in [15].

2.2. Dead-time effects on fluorescence decay curves

In our current paper, we will focus on TCSPC measurements with the recently developed new generation of counting electronics that use independent timers and have a constant dead-time [11]. Although this eliminates classical pile-up effects [8], dead-time effects still distort the recorded fluorescence decay curves. The impact of the dead-times of both detector and electronics is schematically shown in Fig. 1. After each photon detection, the single-photon detector has to recover and is, during some dead-time D, unable to detect another photon. This detector dead-time of length D is symbolized by the small rectangles in Fig. 1. In parallel, after timing a photon detection event, the timing electronics has also to recover, with dead-time E, before being able to record another photon detection event. This dead-time of duration E is symbolized by large rectangles in Fig. 1. Typically, one has $E > D$, but in the case of $E < D$, the problem reduces to a single dead-time problem which is a special case of the theory developed below.
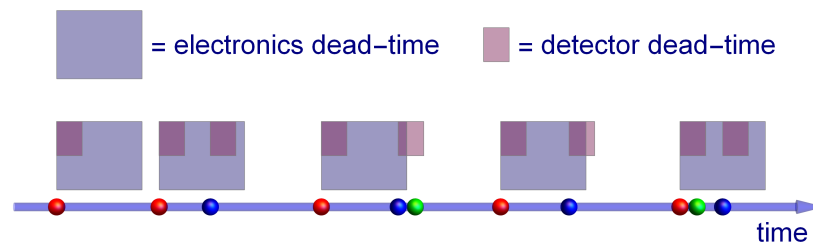

Fig. 1. Schematic of continuous photon detection/registration with dead-time effects of both the electronics (large blue rectangles) and the detector (small violet rectangles). Red balls are successfully detected and recorded photons; blue balls are detected but not recorded photons, because their detection takes place during recovery of the electronics; green balls are photons which hit the detector but are not detected because they fall within the recovery period of the detector. Note that the detector dead-time only occurs after successful detection of a photon (red and blue balls), while the electronics dead-time only occurs after successfully timing a photon (red balls).

Three scenarios for photons hitting the detector are now possible. In the best case, both detector and electronics are in their recovered resting state and can detect and record the photon (red balls in Fig. 1). Or, the detector has already recovered from the previous photon detection event, but the electronics is still in its recovery and not yet ready to record the detected photon (blue balls in Fig. 1). Or, in the worst case, the next photon hits the detector so closely to the previous one that the detector itself is still in its dead-time and cannot detect the photon (green balls in Fig. 1). It is important to notice that this can even happen while the electronics itself would be already capable to record another detection event (see the green photon event in Fig. 1 where the small rectangle, delimiting the detector dead-time, extends beyond the large rectangle, which delimits the electronics dead-time).

Let us now describe mathematically how these dead-times affect a recorded fluorescence decay curve. Consider a fluorescent sample which is excited by a periodic train of short laser pulses with period P. Let us denote the resulting fluorescence photon hit rate (number of photons per time hitting the detector) by $k(t)$. This function is periodic with period P, and its integral over one period is given by $\int_0^P dt' k(t') = \varepsilon P$, where ε is the average rate of detectable photons if there would be no dead-time of neither detector nor electronics. However, due to the dead-time of both detector and electronics, the rate of actually recorded photons $h(t)$ is given
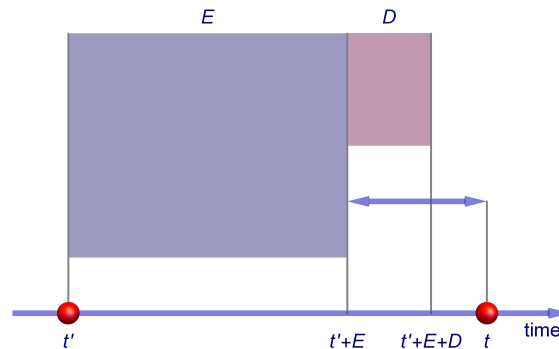
by

$$h(t) = w(t)k(t) \qquad (1)$$

Fig. 2. Schematic of two photon registration events, showing the electronics dead-time (large blue rectangle) and the time region after the electronics dead-time which is still affected by the detector dead-time (small violet rectangle). The double arrow is the time span between the end of the electronics dead-time which started with the last photon registration at time t' and the next photon registration at time t.

where $w(t)$ is a weight function which accounts for the dead-time effects. To find this function, let us consult Fig. 2, assuming that there was a photon detection event at time t'. What is the chance to record the next photon at time t with no other photon recorded in between? Obviously, if $t - t'$ is smaller than the electronics dead-time E, then this chance is zero. If $t - t'$ is larger than $E + D$ so that both electronics and detector have been fully recovered, then this chance is proportional to $\exp[-\int_{t'+E}^{t} d\tau k(\tau)]$, which is the probability that no photon has hit the detector between the time of recovery of the electronics, $t' + E$, and the detection at time t. The situation is slightly more complicated if $t' + E < t < t' + E + D$ because in that case, it is required that there was no photon hitting the detector for the full interval from $t - D$ till t, otherwise the detector would still be in its recovery phase when the next photon arrives at time t. Thus, for this case, the chance is proportional to $\exp[-\int_{t-D}^{t} d\tau k(\tau)]$. One has to multiply this factor by the probability density that there was indeed a photon recording at time t', which is given by $h(t')$ itself. Thus, we arrive for the weight function $w(t)$ at the expression ~~where $w(t)$ is a weight function which accounts for the dead-time effects. To find this function, let us consult Fig. 2, assuming that there was a photon detection event at time t'. What is the chance to record the next photon at time t with no other photon recorded in between? Obviously, if $t - t'$ is smaller than the electronics dead-time E, then this chance is zero. If $t - t'$ is larger than $E + D$ so that both electronics and detector have been fully recovered, then this chance is proportional to $\exp[-\int_{t'+E}^{t} d\tau k(\tau)]$, which is the probability that no photon has hit the detector between the time of recovery of the electronics, $t' + E$, and the detection at time t. The situation is slightly more complicated if $t' + E < t < t' + E + D$ because in that case, it is required that there was no photon hitting the detector for the full interval from $t - D$ till t, otherwise the detector would still be in its recovery phase when the next photon arrives at time t. Thus, for this case, the chance is proportional to $\exp[-\int_{t-D}^{t} d\tau k(\tau)]$. One has to multiply this factor by the probability density that there was indeed a photon recording at time t', which is given by $h(t')$ itself. Thus, we arrive for the weight function $w(t)$ at the expression~~

$$w(t) = \int_{-\infty}^{t-E} dt' h(t') \exp\left[-\int_{\min(t'+E,t-D)}^{t} d\tau k(\tau)\right] \tag{2}$$

where we integrate over all possible recording times t' of the photon preceding the photon at time t. According to the lower bound of the inner integral, we break this into two parts and express the infinite integral as a sum over intervals of length P:

$$w(t) = \int_{t-E-D}^{t-E} dt' h(t') e^{-\int_{t-D}^{t} d\tau k(\tau)} + \sum_{l=0}^{\infty} \int_{t-E-D-(l+1)P}^{t-E-D-lP} dt' h(t') e^{-\int_{t'+E}^{t} d\tau k(\tau)}. \tag{3}$$

Taking into account the strict periodicity of all functions with period P, and that the integral $k(t)$ over one period is εP, a variable transformation $t' \to t' - lP$ for the inner integral of the second part leads to a geometric series, yielding

$$w(t) = e^{-\int_{t-D}^{t} d\tau k(\tau)} \int_{t-E-D}^{t-E} dt' h(t') + \frac{1}{1-e^{-\varepsilon P}} \int_{t-E-D-P}^{t-E-D} dt' h(t') e^{-\int_{t'+E}^{t} d\tau k(\tau)}. \tag{4}$$

Equations (1) – (4) show a very intricate connection between the actual fluorescence decay curves, described by $k(t)$, and the recorded TCSPC curve, given by $h(t)$. These equations determine $h(t)$ via an integral equation involving the product of $h(t)$ and a kernel containing the unbiased decay function $k(t)$.

With Eqs. (1) and (4), one can now calculate the dead-time distorted curve $h(t)$ if the "true" decay curve $k(t)$ is known. One first sets $h(t) = k(t)$, then uses Eq. (4) for calculating $w(t)$, which can be used to update $h(t)$ via Eq. (1), which is then again used to calculate an updated $w(t)$ and so on. This iteration converges already after a few cycles, giving the correct shape of $h(t)$ up to some constant factor. However, the recursion cannot yield the absolute values of $h(t)$, because any re-scaling of $h(t)$ does not change Eq. (1)! Figure 3 shows a Monte Carlo Simulation (MCS) of a TCSPC experiment (see Methods section), together with recursively calculated $h(t)$ which is then linearly fitted against the simulated curve. The figure shows the perfect match between the *shape* of the MCS of $h(t)$ and that of its recursive computation using Eqs. (1) and (4). As can be also seen, the dead-time effects considerably distort the recorded TCSPC curve, mimicking a much faster fluorescence decay at the high-intensity first part of the curve, much faster than the actual decay which underlies the measurement.

Unfortunately, Eqs. (1) and (4) cannot be used to recover $k(t)$ from a measured $h(t)$. The idea would be to first set $k(t)$ equal to $h(t)$, then to calculate $w(t)$ via Eq. (4), which can then be used to update $k(t)$ as $h(t)/w(t)$ following Eq. (1), and so on. However, as we have checked numerically, the result of this procedure depends sensitively on the value of εP which occurs in Eq. (4). If one tries to update this value via $\varepsilon P = \int_0^P k(t) dt$, then the recursion does not converge! Only if this value is known *a priori*, then a recursion using Eqs. (1) and (4) converges to the correct curve $k(t)$. Thus, the next subsection focuses on how to independently determine εP from a measurement.

2.3. Determination of photon hit rate

As we have seen in the previous sub-section, the photon hit rate cannot be obtained from a measured TCSPC curve $h(t)$ and using Eqs. (1) and (4), even if the dead-time values E and D of both electronics and detector are known. However, by using the photon detection raw data, one cannot only calculate the TCSPC curve $h(t)$ by correlating photon detection times with the laser sync, but one can also calculate an Inter-Photon Time Distribution (IPTD) by building a histogram of the time differences of photon detection times between subsequent photons. An experimental example is shown in Fig. 4. Sure enough, the IPTD, which we will denote by $g(T)$, is zero if $T \le E$, due to the electronics dead-time. If $T > E + D$, then the probability
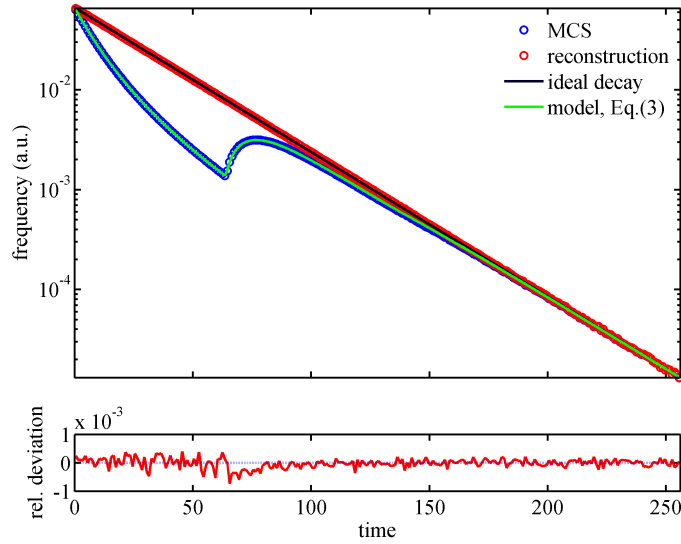
Fig. 3. Monte Carlo Simulation (MCS, blue) of a TCSPC measurement with an excitation period $P = 256$, electronics dead-time $E = 64$, and detector dead-time $D = 16$. The photon hit rate ε was set to a value so that $\varepsilon P = 2$, i.e. that, on average, two photons hit the detector per excitation cycle. The black line shows the underlying perfectly mono-exponential decay curve with a decay time of 30 time units. The green line is the computed $h(t)$ using Eq. (1) and (4) after 10 iterations. The dead-time corrected decay curve, as computed from the simulated $h(t)$, is shown in red. The lower panel shows the relative deviation of the reconstruction (red circles) from the ideal decay (black line), normalized by the square root of the ideal decay.

to detect a next photon at time $t + T$ if there was a detection event at time t is given by the probability of not detecting any photon between the end of the electronics dead-time, $t + E$, and the next photon detection at time $t + T$, times the probability density to see a photon at time $t + T$, i.e. $k(t+T)$. Due to the effect of the detector dead-time, if $E < T \leq E + D$, then this probability is given by the product of the probability of not detecting any photon between $t + T - D$ and $t + T$, and $k(t+T)$. Finally, for finding $g(T)$, one has to average the result over one excitation period with weight function $h(t)$. The result then reads

$$g(T) \propto \int_0^P dt\, h(t) \exp\left[-\int_{\min(E,T-D)}^T d\tau\, k(t+\tau)\right] k(t+T). \qquad (5)$$

The important point now is that, if one sums $g(T)$ over subsequent time intervals $E + D + NP \leq T < E + D + (N+1)P$ of width P, with N being any non-negative integer, i.e. by calculating

$$m_N = \int_{E+D+NP}^{E+D+(N+1)P} g(T)dT = C\exp(-N\varepsilon P), \qquad (6)$$

one finds that these integrals fall off as $\exp(-N\varepsilon P)$, as also shown in Fig. 4. Thus, by fitting the m_N with an exponential function yields the average number of photon hits per excitation cycle, εP. Knowing this number, one can now use Eqs. (1) and (4) to recursively calculate the dead-time-corrected decay $k(t)$ from the measured decay $h(t)$. We have developed a software tool which, for a given file of photon detection times, automatically estimates εP as just described,

and then uses this number for recursively calculating a dead-time corrected TCSPC curve. The tool is public domain and can be downloaded at http://www.joerg-enderlein.de/software.html.
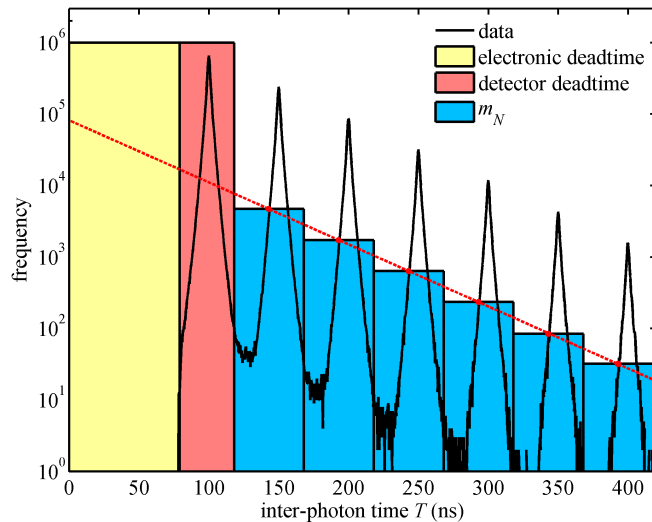

Fig. 4. Measured histogram of the inter-photon time distribution (black solid line) extracted from a TCSPC measurement on a fluorescence dye solution. The yellow and red shaded regions on the left are the electronics and detector dead-time intervals, respectively. The cyan bars are the calculated values of m_N, Eq. (6), for $N = 0, ..., 5$. The red dashed line shows the single-exponential decay of m_N. From this fit, one determines an average value of photon hits per excitation cycle of $\varepsilon P = 1.0$.

2.4. Determination of detector and electronics dead-times

For correctly recovering an unbiased decay curve from a measured TCSPC curve, one needs to know the electronics and detector dead-times, E and D. An elegant way to determine both values is to measure an autocorrelation function while illuminating the measurement system with a *continuous-wave constant-intensity* light source. This autocorrelation function $A(t-t')$ is proportional to the probability of recording a photon at some time t if there was a photon recording at time t'. If the light source has constant intensity (no time-dependence), the auto-correlation function depends only on the time difference $t-t'$.

For deriving a theoretical expression for the autocorrelation function, we will proceed in two steps. In a first step, we completely ignore the dead-time of the electronics and consider only the effect of the dead-time of the detector. Let us consider the probability density to record a photon at time t if there was a photon recording at time t', but no photon recording in between. Obviously, this probability density is zero if $t-t' \leq D$, and if $t > t'+D$, then it will be proportional to $\exp[-\varepsilon(t-t'-D)]$, which is the probability that no photon hits the detector between time $t'+D$ and time t, and ε is the constant average photon hit rate. Thus, the normalized probability density $f(t-t')$ for detecting a photon at time t if there was a detection event at time t' with no other photon detection in between is given by

$$f(t) = \begin{cases} 0 & \text{if } t \leq D \\ \varepsilon \exp[-\varepsilon(t-D)] & \text{if } t > D. \end{cases} \tag{7}$$

Next, let us consider the same probability density but now with exactly one intermediate photon recorded at any time t'' in between. Obviously, this probability density is zero if $t - t' \leq 2D$, and is otherwise equal to the auto-convolution of the probability density $f(t)$, $\int_0^t dt'' f(t - t'') f(t'')$, computed at time $t - t' - 2D > 0$. By repeating this argument for all possible numbers of intermediate photon recordings, one finds the following expression for the autocorrelation function $a(t)$ [16]:

$$a(t) = \sum_{j=1}^{\lfloor t/D \rfloor} f^{(j)}(t) \tag{8}$$

where $f^{(j)}(t)$ is the j-th auto-convolution of the function $f(t)$ which is recursively defined by

$$f^{(j)}(t) = \int_0^t dt' f(t') f^{(j-1)}(t - t') \tag{9}$$

and setting $f^{(1)}(t) = f(t)$. The upper limit in the summation (8) is the maximum possible number of photons which can be recorded within time t for a given detector dead-time D, where $\lfloor t/D \rfloor$ denotes the largest integer number smaller than t/D.

Now we are ready to consider the general case of both detector and electronics dead-time, assuming that $D \leq E$ (the case $D > E$ reduces to the just considered case of a system having only detector dead-time D). Analogously to the derivation of $a(t)$, we will again start by finding an expression for the normalized probability density $F(t - t')$ to detect a photon at time t if there was a photon detection at time t' but no other photon detection in between. Due to the electronics dead-time, this probability density is zero if $t - t' < E$. The interesting case now occurs if $t - t' > E$ but also $t - t' < E + D$. In that case, it can happen that a photon hits the detector shortly before the electronics recovers from its own dead-time so that no photon can be detected due to the detector dead-time although the electronics is again ready to process another detection event, see also Figs. 1 and 2. For this intermediate time interval, $E < t - t' < E + D$, the function $F(t - t')$ is proportional to the previously found autocorrelation $a(t - t')$ which is exactly the chance to be able to see another photon at t if there was one at time t', when taking into account the detector dead-time alone. Finally, for time values t greater than $t' + E + D$, the probability density F will fall off exponentially as $\exp[-\varepsilon(t - t' - D - E)]$, which is the probability that no photon hits the detector between time $t' + E + D$ and time t. In summary, we find

$$F(t) = \begin{cases} 0 & \text{if } t \leq E \\ Z^{-1} a(t) & \text{if } E < t \leq E + D \\ Z^{-1} a(E + D) \exp[-\varepsilon(t - E - D)] & \text{if } t > E + D \end{cases} \tag{10}$$

where Z is a normalizing constant, and $a(t)$ is taken from Eq. (8). By a similar reasoning as before, the final autocorrelation function $A(t)$ is then found as

$$A(t) = \sum_{j=1}^{\lfloor t/E \rfloor} F^{(j)}(t) \tag{11}$$

where $F^{(j)}(t)$ is the j-th auto-convolution of the function $F(t)$, and the upper limit in the summation (11) is the maximum possible number of photons which can be recorded within time t when taking into account the electronics dead-time E.

Thus, the calculation of the full autocorrelation function, Eq. (11), starts first by calculating the function $f(t)$, Eq. (7), using the knowledge of the detector dead-time D and the average photon hit rate ε; then continues by calculating $a(t)$, Eq. (7), via recursive convolutions of
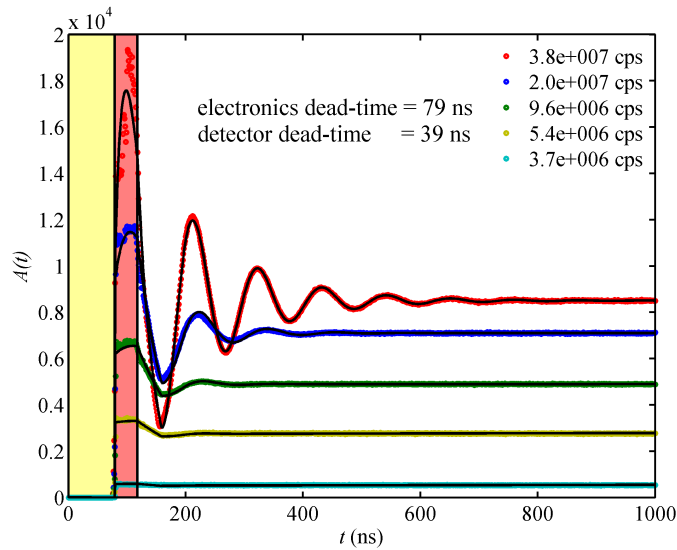
Fig. 5. Autocorrelation functions for five different photon hit rates ε as indicated in the legend. Measured curves are represented by circles, solid lines show a global fit of Eq. (11) to all five measurements. The yellow and red shaded regions on the left mark the fitted electronics and detector dead-times, respectively. All autocorrelation functions were calculated at evenly spaced time points with 1 ns spacing. At very high count rates, fit quality starts to deteriorate due to increasing jitter of the detector dead-time.

$f(t)$, Eq. (9); then proceeds by calculating $F(t)$, Eq. (10), using $a(t)$ and the knowledge of the electronics dead-time E; and ends by calculating the final autocorrelation functions $A(t)$ via recursive convolutions of $F(t)$. Although this may seem computationally expensive, it is not: The numerical calculation for one autocorrelation function with ca. 1000 sampling points along the time axis needs only a fraction of a second on a conventional PC and using a non-compiled *Matlab* script, which is included in our dead-time correction toolbox which can be downloaded at http://www.joerg-enderlein.de/software.html. Thus, it can be easily used for fitting measured autocorrelation curves and thus for extracting D, E and ε as fit parameters. An example for five different count rates is shown in Fig. 5, using our experimental TCSPC system (see Methods section) with the laser in continuous wave mode. The sample was a dye solution of Atto655 as described in section 3.2. Autocorrelation curves of different count rates were fitted with a global model for E and D, but individual values for εP. From the fitted curves, we determined a detector dead-time of $D = (39.5 \pm 0.6)$ ns (red shaded region in Fig. 5), and an electronics dead-time of $E = (79.1 \pm 0.4)$ ns (yellow shaded region in Fig. 5). The errors were obtained by bootstrapping the data into 14 bunches of 10^6 photons each and calculating mean and standard deviation.

3. Results

3.1. *Numerical simulation of dead-time correction*

To check the performance of our algorithm of reconstructing an unbiased TCSPC curve from one with dead-time effects, we performed Monte Carlo simulations. All simulations were done with the same electronics and detector dead-time values as used for Fig. 3, and by assuming again a perfectly mono-exponential decay with a decay time value of 30 time units. It should be
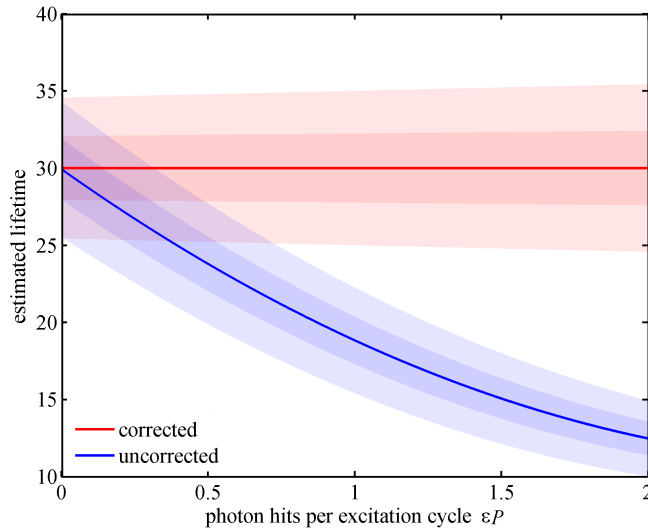
Fig. 6. Results of Monte Carlo simulations of the performance of the recovery algorithm for dead-time corrected decay curves from measured TCSPC. Shown are the mean values (solid lines) and variances (shaded regions) of mono-exponential decay time values which are obtained from fitting the simulated decay curves. Simulations were performed for the same dead-time values as used in Fig. 3, for a range of photon hit values per excitation period, εP, from zero to 2, and for two different values of total number of photon hits, i.e. εP times number of excitation cycles, of 200 (light shaded region) and 1000 (dark shaded region). The corresponding decay curves have smaller number of photons, due to the dead-times of both electronics and detector.

emphasized that the particular character of the decay is completely unimportant, because our algorithm will reconstruct an unbiased TCSPC curve whatever the underlying decay curve is, and it is completely independent of the particular nature of this decay. In the simulations, we assumed that the number of photons per sufficiently small time interval Δt centered at time t is described by a Poissonian probability distribution with mean value $k(t)\Delta t$. Simulations were performed for two values of total photon hits of 200 and 1000 photons, respectively, and for a range of average photon hits per excitation, εP, between zero and two. It should be mentioned that the actual number of *counted* photons, $\varepsilon' P = \int_0^P h(t)dt$, becomes increasingly smaller, with increasing value of εP, than the number of total photon hits due to dead-time effects.

For each simulated experiment, we calculated the "measured" decay curve, $h(t)$, and the IPTD, $g(T)$, from which the values m_N were calculated, see. Eq. (6). From these values, an estimate of εP was derived by fitting the m_N to an exponential function in N. This estimate was then used in the reconstruction of the dead-time corrected decay $k(t)$ from $h(t)$, using Eqs. (1) and (4). Finally, both $h(t)$ and $k(t)$ were fitted with a mono-exponential decay function for determining the decay time. For each pair of values of total photon hits and εP, we performed 10^4 simulations, and we then fitted the resulting decay-time distributions by Gaussians, for obtaining the mean value and variance of the decay-time estimation. The final result of these simulations is summarized in Fig. 6. It shows for both the raw and dead-time corrected decay curves the mean value and variance of the extracted decay-time value as a function of the average number of photon hits per excitation cycle, εP. As can be seen, with increasing value of εP, the dead-time distortion of the "measured" decay curve $h(t)$ leads to increasingly shorter

apparent decay times. However, when fitting the dead-time corrected decay-curves, one finds perfect agreement, on average, between the fitted and the actual decay-time. Remarkably, the dead-time correction even works well for as few as only 100-200 photons per measured decay curve. Only the variance of the fitted decay-times becomes wider for smaller numbers of total photon counts, but no systematic bias in the decay-time estimate is showing up.

3.2. Fluorescence decay measurements on dye solution

As a first experimental proof of principle of the validity and performance of our reconstruction algorithm, we recorded TCSPC data on a sample of a pure dye solution, where we changed, from measurement to measurement, the excitation intensity and thus the impact of dead-time effects. A thick dye solution ($10\,\mu M$) of Atto655 (ATTO-TEC, Siegen, Germany) in combination with a variable laser power was used to generate different photon hit rates ε. For very high photon hit rates ($\varepsilon \gtrsim 1/P$), buffer overruns were encountered after a few seconds, but during that time, a sufficiently large number of photons could be recorded. TCSPC histograms were constructed from the photon arrival times. For all histograms, we used bunches of 10^6 photons, and for the dead-time correction we used the *a priori* determined dead-time values $E = 79\,ns$ and $D = 39\,ns$. For each measurement, the parameter εP was estimated from the IPTD of photon arrival times, separately for each bunch. Lifetimes were determined by tail-fitting, starting 1 ns after the peak of the decay curve, and using a mono-exponential fit function and a simplex fitting routine. This procedure was repeated for ten consecutive bunches of 10^6 photons each, yielding an average εP and an average lifetime with standard deviation for each measurement, which are plotted in Fig. 7. As can be seen from this plot, the dead-time distortion effect leads to a decrease in fitted lifetime of the uncorrected histograms with increasing excitation rate, i.e. number of photon hit per excitation cycle εP. The figure also shows that the dead-time correction results in fitted lifetime values which are unbiased and independent of εP, with an unbiased lifetime value of $\tau_{fl} = (1.902 \pm 0.005)\,ns$ (dashed line), in excellent agreement with published lifetime values of Atto655.

3.3. Fluorescence lifetime imaging

We performed FLIM measurements of fixed human mesenchymal stem cells with actin filaments labeled with the dye Atto647N. The sample was imaged with a home-built confocal microscope using a 640 nm excitation laser and a long-pass filter before the detector. Results are shown in Figs. 8 and 9. Both intensity and lifetime images are shown, with and without dead-time correction. In particular for the high-intensity images, the dead-time correction shows a clear improvement and rectification of both intensity and lifetime values. Even for the low-intensity image, where the excitation intensity was reduced by six times and the maximum number of photon hits per excitation cycle was well below 0.1, one can still see slight changes in lifetime values after dead-time correction. In the top row of Fig. 10, we show a line plot through the brightest pixel of Fig. 8. The bright pixels (upper left plot) show a significantly lower lifetime in the uncorrected data (upper right plot) due to dead-time distortion. This trend is not visible after the correction: the lifetime stays constant over the line within the statistical error. Thus, in this case, not correcting for the dead-time distortions would lead to misinterpretation of the data. In the bottom row of Fig. 10 we show the TCSPC histograms of the brightest pixel at high (bottom left, $\varepsilon P = 0.50$) and low laser power (bottom right, $\varepsilon P = 0.09$). One can clearly see that the uncorrected and corrected TCSPC curves show a negligible difference for the lower photon hit rate, which is clearly not the case for the curves shown for the high εP value. The fitted lifetime values of the corrected curves agree within their errors, whereas the values differ significantly for the uncorrected curves.
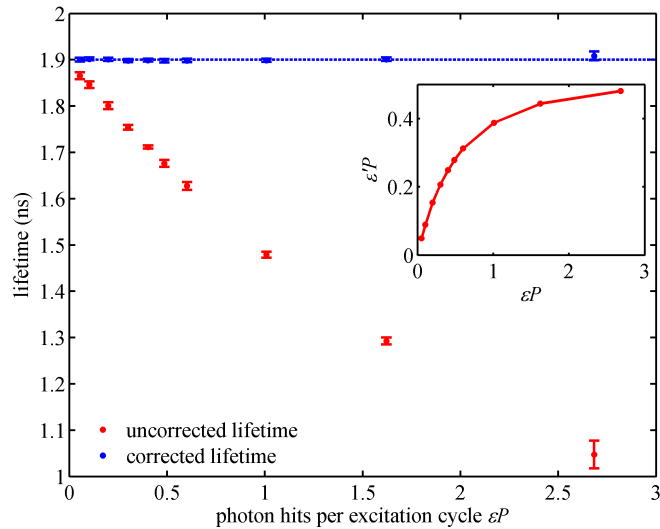
Fig. 7. TCSPC measurements on Atto655 dye solution at varying excitation power and thus fluorescence intensity. The fluorescence intensity is given here as dead-time corrected values of average number of photon hits per excitation cycle, εP. The inset shows also the relation between the actual average number of detected photons per excitation cycle, $\varepsilon' P$, and εP, showing the increasing dead-time related saturation of the measurement system with increasing intensity. Red symbols show determined lifetime values from uncorrected TCSPC curves, and blue symbols show lifetime values determined from dead-time corrected TCSPC curves. The dashed line shows the average over all lifetime values for all dead-time corrected measurements.

4. Methods

4.1. Monte Carlo simulations

Monte Carlo simulations of the TCSPC experiment were performed in the following way. First, for each excitation cycle, the number of hitting photons was randomly drawn from a Poissonian distribution with mean value εP. Then, for the thus determined number of photons, their hit times with respect to the start of the corresponding excitation cycle were randomly drawn from an exponential distribution with decay time τ, where τ is the value of the mono-exponential fluorescence decay one wants to model. Knowing the excitation cycle and the hit time within this cycle for each photon, the global hit time is calculated for each photon, and then all these times are sorted in time. Then, the algorithm steps sequentially through these photon hit times and determines, for each photon, whether its hit time is still within the detector or electronics dead-time interval of the previous validated photon detection event. If this is the case, then the photon is eliminated from the photon stream, and the algorithm proceeds to the next photon. Finally, from the remaining photon stream, a TCSPC histogram and the IPTD is calculated.

4.2. Software

The software for the dead-time correction of fluorescence lifetime measurements used in this study is available for download at http://www.joerg-enderlein.de/software.html. It is written in *Matlab* with core parts outsourced to C++ MEX files for performance acceleration, which can be compiled under Windows or Linux using the provided build scripts. The algorithm recovers
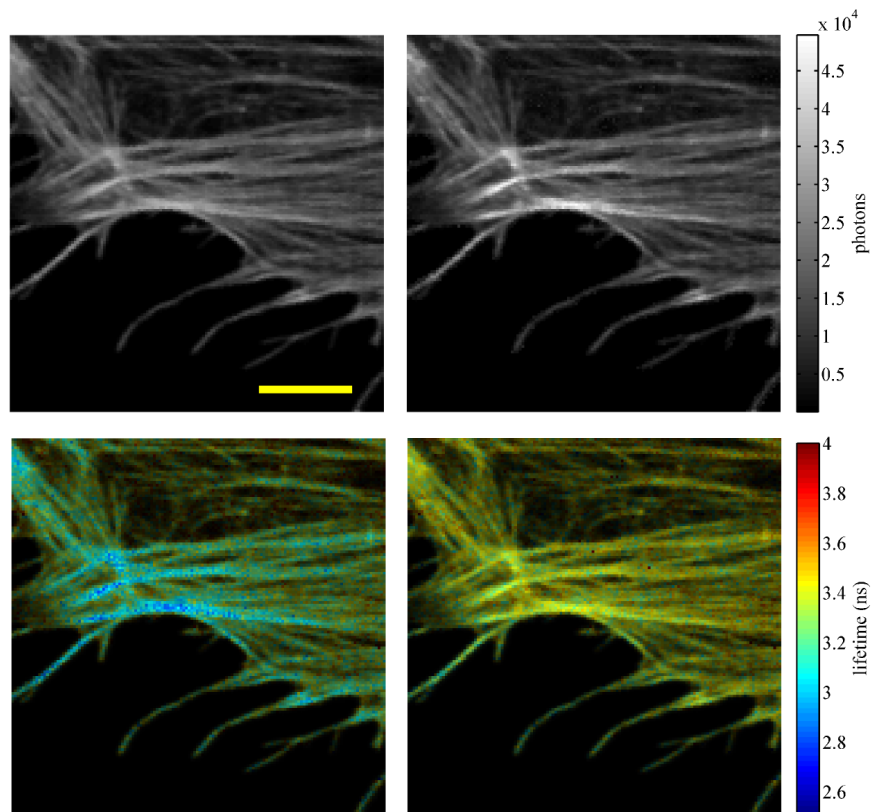
Fig. 8. Human mesenchymal stem cell with actin filaments labeled by Atto647N, and imaged with a confocal scanning TCSPC microscope. The top row shows the intensity image before (left) and after (right) dead-time correction, where the counts were determined using the calculated hit rates (ε) for each pixel. One can clearly see the significant increase in signal strength after dead-time correction for regions with high fluorescence intensity. The bottom row shows the same for the lifetime images (left before, and right after dead-time correction). The tremendous impact of artifacts on the resulting lifetimes is clearly visible: In regions of high intensity, the lifetime values in the left bottom image always underestimate the true value, as seen in the dead-time corrected image at bottom right. The images are $20 \times 20\,\mu\mathrm{m}^2$ with a pixel size of $140\,\mathrm{nm}$ and a dwell time of $5\,\mathrm{ms}$ per pixel, the yellow scale bar is $5\,\mu\mathrm{m}$. The highest number of photon hits per excitation cycle in this image is 0.5.
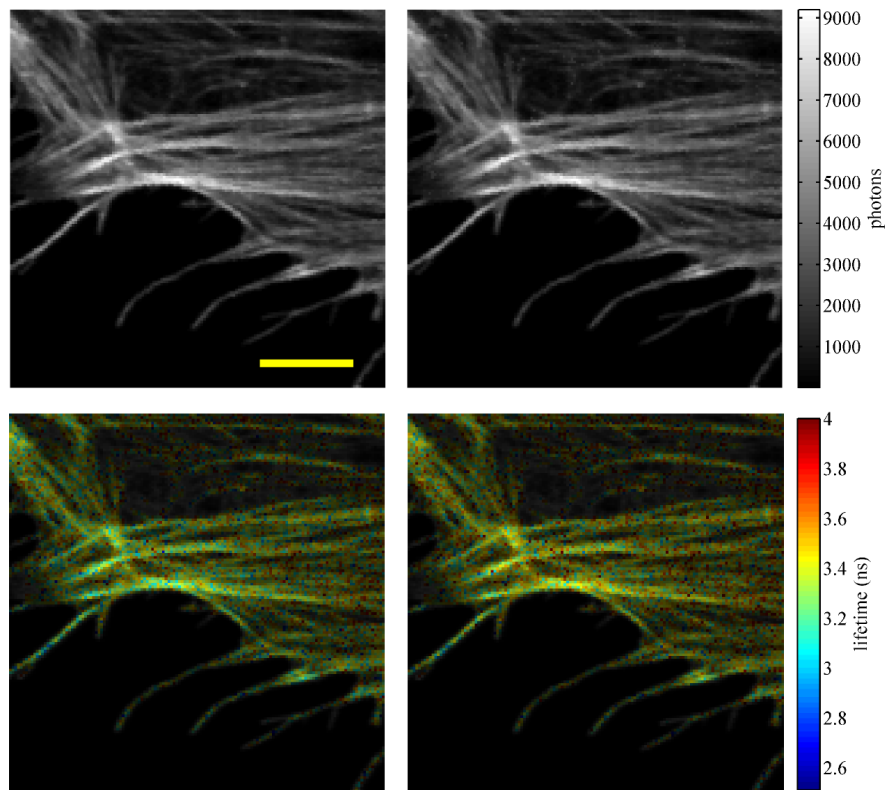
Fig. 9. Image of the same sample as in Fig. 8, but using a ca. six times lower excitation intensity. Now, the dead-time correction does nearly not change neither the intensity nor the lifetime images, and both lifetime images are close to the dead-time corrected lifetime image of Fig. 8. However, due to the much lower fluorescence signal strength, the lifetime image is much noisier than the dead-time corrected lifetime image in Fig. 8.

the true photon hit rate $k(t)$ from the measured curve $h(t)$ in an iterative fashion, starting from the guess $k_0(t) = h(t)$. In a next step, $w_0[t|k_0(t)]$ is computed via Eq. (4), and it is used to update $k(t)$ as $k_1(t) = h(t)/w_0[t|k_0(t)]$. This is repeated n times, until the relative change in $k_n(t)$ is smaller than a predefined threshold. It was observed that convergence is usually fast requiring only about 2 to 5 iterations.

4.3. Setup for cell measurements

For FLIM measurements, we used a setup based on a commercial confocal system (Microtime 200, PicoQuant, Berlin, Germany). Linearly polarized light from a 640 nm diode laser (LDH-D-C-640, PicoQuant, Berlin, Germany), equipped with a clean-up filter (Z640/10, Chroma Technology, Rockingham, VT, USA), was coupled into a polarization-maintaining single mode optical fiber. The laser driver (PDL 828 "Sepia II", PicoQuant, Berlin, Germany) allows for continuous wave (cw) or pulsed excitation mode of the laser (pulse width of 100 ps FWHM). For all lifetime measurements, we used the pulsed excitation mode with a repetition rate of 20 MHz. The light at the fiber output was re-collimated and reflected by a dichroic mirror (FITC/TRITC Chroma Technology, Rockingham, VT, USA) into the side port
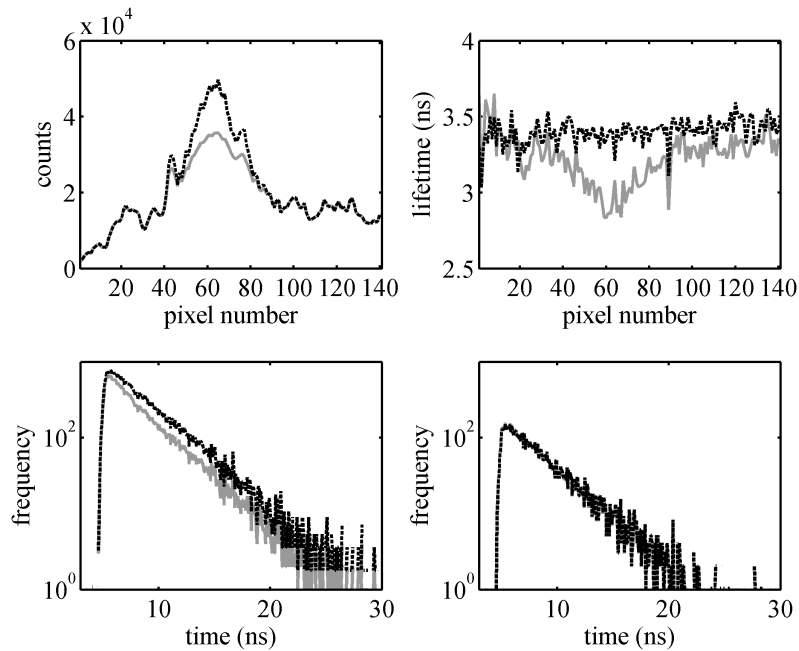
Fig. 10. The upper row shows a line plot through the brightest pixel of the cell measured at high laser power (Fig. 8) for intensity (left) and lifetime (right). The TCSPC curve of the brightest pixel ($\varepsilon P = 0.50$) is given in the lower left plot yielding $\tau_{\text{uncorrected}} = (2.87 \pm 0.02)\,\text{ns}$ and $\tau_{\text{corrected}} = (3.42 \pm 0.02)\,\text{ns}$. Next to it on the right, the TCSPC curve of the same pixel at low laser power (Fig. 9) is shown ($\varepsilon P = 0.09$), yielding $\tau_{\text{uncorrected}} = (3.36 \pm 0.04)\,\text{ns}$ and $\tau_{\text{corrected}} = (3.47 \pm 0.04)\,\text{ns}$. For all plots, the gray line represents the uncorrected data and the dashed black line the corrected data.

of an inverted microscope (IX71, Olympus Deutschland, Hamburg, Germany). An internal mirror reflected the beam into the back aperture of the objective (UPLSAPO 100× Oil, 1.4 N.A., Olympus Deutschland, Hamburg, Germany), which also collected the fluorescence light. After a 50 μm pinhole, the light was collimated and focused onto a single-photon counting module (SPCM-CD 3516 H, Excelitas Technologies, Wiesbaden, Germany). Back-scattered excitation light was blocked with a long-pass filter (EdgeBasic BLP01-635R, Semrock, Rochester, NY, USA). A single-photon timing electronics (HydraHarp 400, PicoQuant, Berlin, Germany) was used to record the detected photons with an absolute temporal resolution of two picoseconds. The sample was mounted on a three-axis piezo stage (P-562.3CD with controller E-710.3CD, both Physik Instrumente, Berlin, Germany), and image acquisition was performed using the SymphoTime software (PicoQuant, Berlin, Germany) in time-tagged, time-resolved (TTTR) mode.

4.4. Setup for solution measurements

For the solution measurements, the same setup as described in the previous subsection was used, but with few modifications: We used a water immersion objective (UPLSAPO 60×W, 1.2 N.A., Olympus Deutschland, Hamburg, Germany) and a 150 μm pinhole and a band-pass filter (BrightLine HC 692/40, Semrock, Rochester, NY, USA). For data acquisition, the output of the detector was connected to an inverter (SIA 400, PicoQuant, Berlin, Germany) followed

by the timing electronics (HydraHarp 400, PicoQuant, Berlin, Germany). There, events were recorded with 32 ps resolution with respect to the 20 MHz sync signal provided by the laser driver. The timing data was recorded with the original HydraHarp 400 software (version 3.0) in TTTR mode. For the measurement of the autocorrelation function, the laser was used in cw mode.

4.5. Cell culture and staining

Adult human mesenchymal stem cells from bone marrow (hMSCs, P4, Lonza, PT-2501), have been cultivated in T75 cell culture flasks (Corning, 43061) in DMEM (Gibco, A18967-01), 10% fetal bovine serum (Sigma-Aldrich, F2442-500ML) and 1% antibiotics (Penicillin/Streptomycin, life technologies, 15140-122) at 37°C and 5% CO_2 and split every 2-3 days (P2→P4). Then the cells were seeded on glass cover slides in a density of 10.000 hMSCs per glass in 6-well plates (Sarstedt, 83.3920). They were supplied with 2 ml medium/well at 37°C and 5% CO_2. The cells have been fixed 24 h after seeding using 10% Formaldehyde in PBS for 5 min. The cells were permeabilised using 0.5% Trition X 100 in PBS for 10 min, blocked with 3% BSA in PBS for 30 min, incubated in Triton X for 5 min and washed with PBS. All antibodies were kept in 3% BSA in PBS. Fluorescent staining was performed with Phalloidin Atto647N (Atto-Tec, AD647N-82) [1:250] for 1.5 h. The samples were mounted on microscope slides (VWR, 631-1550) using Fluoroshield mounting medium (F6182-20ML).

5. Conclusion

We have presented a complete analysis of dead-time effects in TCSPC measurements, and have developed an algorithm for how to correct these effects in measurements. It is important to emphasize that the correction algorithm is very general and does not depend, in any way, on the particular nature of the underlying fluorescence decay. It is applicable to any single-event counting or timing measurement with electronics and/or detector dead-times and is not restricted to TCSPC measurements. It not only corrects dead-time artifacts for lifetime, but also for intensity, which could be beneficial for lidar [17] or time-resolved fluorescence anisotropy measurements [18]. We have written a free software for *Matlab* which can be downloaded at http://www.joerg-enderlein.de/software.html. We hope that the correction scheme will find wide application in all TCSPC measurements where high count rates are encountered, in particular in high-speed FLIM measurements.

In principle, it should be possible to extend the model to reverse start-stop TCSPC. One would have to include the pile-up and variable dead-time by making the dead-time a function of the photon arrival time. However, our present model should theoretically also be applicable to a reverse start-stop TCSPC system as long as the dead-time of the system is constant and longer than the excitation period.